352. Low-frequency acoustic instability of the working process in the combustion chamber of the solid propellant rocket engine

Yu. M. Davydov, M. Yu. Egorov
Institute of Mechanics and Ecology,
Moscow, Russia,
E-mail: *1presidium@bk.ru*

(Received 2 April 2008; accepted 13 June 2008)

Abstract: The following problems is investigated by statement of direct numerical experiment in offered paper.
1) The real oscillatory process is reproduced.
2) The mechanism of occurrence and refill of low-frequency acoustic instability in the combustion chamber of the solid propellant rocket..

The direct numerical modeling of low-frequency acoustic instability will be carried out by a Davydov's method. This powerful numerical method was discovered by Yuri M. Davydov 40 years ago as the method of large particles The further modern complex improvement of this numerical technique was titled Davydov's method. It is good itself recommending at the decision of many tasks of the mechanics of continuous media. The description of physical and mathematical model of flow in the rocket engine combustion chamber is given.

The results of numerical modeling are resulted. The hydrodynamical deeply nonlinear nature of low-frequency fluctuations connected to structure and character of current in the combustion chamber of the solid propellant rocket engine proves to be true.

Keywords: acoustic instability, vibrations, rocket engine, low frequency, combustion chamber.

Notation

$A -$ amplitude of fluctuations;
$a -$ sound speed;
$alfa -$ parameter of finite-difference scheme;
$beta -$ parameter of finite-difference scheme;
$c -$ specific heat capacity, factor of resistance;
$d -$ diameter;
$E -$ full specific energy;
$f -$ frequency of pressure fluctuations (pulsations);
$G -$ drain-arrive complex;
$J -$ specific internal energy;
$k -$ adiabatic parameter;
L – length (characteristic size);
$n -$ number of particles in unit of volume;
$p -$ pressure;
$q -$ thermal interphase interaction function;
$r -$ coordinate along an axis 0R, radius;
$s -$ area;
$T -$ temperature;
$t -$ time;
$u -$ velocity along axis 0X;
$V -$ volume;
$v -$ speed along axis 0У (0R), burning speed of solid propellant;
$\mathbf{W} -$ speed vector;
$W -$ module of a speed vector, speed of submission of products of combustion from a surface of burning;
$x -$ coordinate along axis 0X;
α - share of volume occupied by i phase of a mix;
γ – main angle;
λ - heat conductivity factor;
μ - dynamic viscosity factor;
ν - parameter in the burning law, mass share of a firm phase;
ρ - density;
τ - function of force interphase interaction;

Acronyms

SPRE – solid propellant rocket engine.

Symbols

$g -$ gas;
$i -$ number, index;
$j -$ number, index;
$n -$ number, index;
$p -$ particles in combustion products, parameter dependent on pressure;
$r -$ along axis 0R;

$w -$ burning surface;
$x -$ along axis 0X;
$tm -$ true meaning;
$1 -$ the first phase of a heterogeneous mix;
$2 -$ the second phase of a heterogeneous mix;
$* -$ special value.

Vibration of rocket engines is important part of vibroengineering. Academician K. M. Ragulskis occupies fundamental part in vibroengineering [1, 2 etc.].

The problem of instability of working process in its various manifestations arose simultaneously with the beginning of development and operation of the first solid propellant rocket engines (SPRE) [3, 5, 6 etc.] (and not only solid propellant [4-6 etc.]). Currently due to the development of rocket engines of the new generation with high energomass, operational and other characteristics the significance of a problem has increased.

The instability of the working process in SPRE generally can have acoustic and non-acoustic highly nonlinear nature [5, 6 etc.]. The acoustic instability (this kind of instability is considered in this work) is connected to occurrence of periodic low- and high-frequency pressure fluctuations in the combustion chamber of the engine. The low-frequency pressure fluctuations with provisional range of frequencies $f \approx 20-2000 Hz$ are manifested basically in a longitudinal direction of the combustion chamber. The high-frequency pressure fluctuations with a range of frequencies $f > 2000 Hz$ are observed in transverse and tangential directions of the combustion chamber.

The low-frequency acoustic instability of operations mode of the solid propellant rocket engine has a hydrodynamic (gas-dynamic) highly nonlinear nature, which is convincingly confirmed by experimental (nature and laboratory) and theoretical research [7-12 etc.]. The most significant contribution to low-frequency acoustic instability is brought by the work of inertia - mass forces of a combustion products flow at its irregular interaction with the combustion chamber and the nozzle. The high-frequency instability is more often a consequence of the interaction of resonant waves that are generated in the combustion chamber of the rocket engine with a burning surface of a charge of firm propellant [5, 6].

The greatest danger is represented by the low-frequency acoustic instability of the working process in SPRE. Such type of instability is characterized by a significant deviation of the working pressure in the combustion chamber from the average meaning, it breaks the settlement operation mode of nozzle, initiates transfer of periodic oscillatory loadings from the engine to the rocket system as a whole, it is a source of intensive unmasked noise, etc.

Currently the occurrence of low-frequency acoustic instability in the solid propellant rocket engine is hardly predicted and not amenable to the direct numerical simulation (the real oscillatory process is not reproduced in the simulation). There are only indirect approximate estimation techniques of the occurrence of pressure fluctuations in engines of a specific typical design [8, 9]. The developers of rocket engineering are compelled to eliminate the given type of instability due to the experimental improvement of the rocket engine design by a trial and error method.

In this work and in [10-12] for the first time the application of direct numerical experiment enables reproduction of real oscillatory process and the mechanism of occurrence and the refill of the low-frequency acoustic instability in the combustion chamber of SPRE is investigated. The direct numerical modeling of the low-frequency acoustic instability in the solid propellant rocket engine is carried out by the method of Davydov (the method of large particles) [13, 14 etc.]. This method has been successfully applied for solution of many nonlinear problems of mechanics of continuous media [10, 12, 15 etc.].

The approaches of the mechanics of continuous multiphase media are applied to the description of process of the current in the combustion chamber and the nozzle of SPRE [16 etc.]. Gas combustion products of solid propellant constitute the first phase, firm burned down particles (oxide of aluminium) – the second phase. The first and the second phases are considered as a heterogeneous mix with the determined temperatures and speeds of movement. In such system each phase occupies a part of volume of a mix: $\alpha, (1-\alpha)$. Their movement is considered as the movement of interpenetrative and cooperating environments.

In addition for the simulated task we accept the following assumptions: (a) from the spatial point of view we study the process of current as 2D axi-symmetric; (b) we consider gas products of combustion as the ideal completely reacted gas; (c) the reburning metallic firm phase (particles of aluminium) in the combustion chamber of the engine is not taken into account; (d) gluing and splitting of the burned down firm phase (oxide of aluminium) during the movement in the combustion chamber and the nozzle are not taken into account as well.

In view of the assumptions listed above, the complete non-stationary system of the vortical differential equations of gas dynamics for heterogeneous flow in the combustion chamber and the nozzle of a solid propellant rocket engine have the following form:

- the equations of indissolubility (preservation of mass)

$$\frac{\partial \rho_1}{\partial t} + div(\rho_1 \mathbf{W}_1) = G_{gw}; \qquad \frac{\partial \rho_2}{\partial t} + div(\rho_2 \mathbf{W}_2) = G_{pw}; \tag{1}$$

- the equations of preservation of a pulse on coordinates axes

$$\frac{\partial(\rho_1 u_1)}{\partial t}+div(\rho_1 u_1 \mathbf{W}_1)+\alpha\cdot\frac{\partial p}{\partial x}=-\tau_x+W_x\cdot G_{gw};$$
$$\frac{\partial(\rho_1 v_1)}{\partial t}+div(\rho_1 v_1 \mathbf{W}_1)+\alpha\cdot\frac{\partial p}{\partial r}=-\tau_r+W_r\cdot G_{gw};$$
$$\frac{\partial(\rho_2 u_2)}{\partial t}+div(\rho_2 u_2 \mathbf{W}_2)+(1-\alpha)\cdot\frac{\partial p}{\partial x}=\tau_x+W_x\cdot G_{pw};$$
$$\frac{\partial(\rho_2 v_2)}{\partial t}+div(\rho_2 v_2 \mathbf{W}_2)+(1-\alpha)\cdot\frac{\partial p}{\partial r}=\tau_r+W_r\cdot G_{pw};\tag{2}$$

- the equations of preservation of specific energy

$$\frac{\partial(\rho_2 J_2)}{\partial t}+div(\rho_2 J_2 \mathbf{W}_2)=q+J_{pw}\cdot G_{pw};$$
$$\frac{\partial(\rho_1 E_1)}{\partial t}+\frac{\partial(\rho_2 E_2)}{\partial t}+div(\rho_1 E_1 \mathbf{W}_1)+div(\rho_2 E_2 \mathbf{W}_2)+$$
$$div(\alpha p \mathbf{W}_1)+div[(1-\alpha)p\mathbf{W}_2]=J_{gw}\cdot G_{gw}+J_{pw}\cdot G_{pw},\tag{3}$$

- where for axi-symmetric case

$$div(\varphi \mathbf{W}_i)=\frac{\partial(\varphi u_i)}{\partial x}+\frac{1}{r}\cdot\frac{\partial(r\varphi v_i)}{\partial r},$$
$$\varphi=[\rho_i,\rho_i u_i,\rho_i v_i,\rho_2 J_2,\rho_i E_i,\alpha p,(1-\alpha)p];$$
$$i=(1,2).$$

The kind of system (1) - (3) is identical both for dimensional and non- dimensional units. Further we will use the latter, having taken characteristic parameters, for example, parameters of braking for the given engine. Density ρ_i we will relate to ρ_*; speed (in projections on coordinate axes) u_i, v_i - to sound speed at parameters of braking a_*; pressure p - to $\rho_*\cdot a_*^2$; specific energy (both internal, and complete) J_2, E_i - to a_*^2; linear units - to the characteristic size of the combustion chamber L; time t - to L/a_*.

To close the system of the differential equations (1) - (3) we will use the equation of condition as:

$$p=(k-1)\cdot\rho_1^{tm}\cdot\left(E_1-\frac{W_1^2}{2}\right).\tag{4}$$

Let's describe the kind of the right-hand sides of the equations (1) - (3). The arrival of combustion products from the burning surface of a charge of solid propellant are defined as:

$$G_{gw}=(1-\nu)\cdot s_w\cdot v_{k_w}\cdot\rho_w^{tm}\cdot\frac{1}{V};$$
$$G_{pw}=\nu\cdot s_w\cdot v_{k_w}\cdot\rho_w^{tm}\cdot\frac{1}{V},\tag{5}$$

where the burning speed of solid propellant is determined on experimental dependence $v_{k_w}=f(p,dp/dt,W)$.

The speed (in projections to coordinate axes) receipt of combustion products (gas + firm particles) from the burning surface of a charge of solid propellant in the chamber of the engine is defined as:

$$W_x=v_{k_w}\cdot\rho_w^{tm}\cdot\frac{1}{\rho_*}\cdot\frac{tg\gamma}{\sqrt{1+tg^2\gamma}};$$
$$W_r=-v_{k_w}\cdot\rho_w^{tm}\cdot\frac{1}{\rho_*}\cdot\frac{1}{\sqrt{1+tg^2\gamma}},\tag{6}$$

where γ - the corner between tangent to the burning surface and the positive direction of the axis 0X.

Calorific ability of solid propellant combustion products (gas + firm particles) is defined as:

$$J_{gw}=\left(c_p-\frac{c_p}{k}\right)\cdot T_*\cdot\frac{1}{k-1};$$
$$J_{pw}=c_2\cdot T_*.\tag{7}$$

The expression for function of power interphase interaction, caused only by superficial friction, is defined by the formulas:

$$\tau_x=n\cdot\pi\cdot d_p^2\cdot\rho_1^{tm}\cdot c_x\cdot|\mathbf{W}_1-\mathbf{W}_2|\cdot(u_1-u_2)\cdot\frac{1}{8};$$
$$\tau_r=n\cdot\pi\cdot d_p^2\cdot\rho_1^{tm}\cdot c_r\cdot|\mathbf{W}_1-\mathbf{W}_2|\cdot(v_1-v_2)\cdot\frac{1}{8}.\tag{8}$$

Factor of resistance in (8), for example, is calculated as:

$$c_x=\frac{24}{\mathrm{Re}}+\frac{4}{\mathrm{Re}^{0,33}},\qquad \mathrm{Re}\le 700;$$
$$c_x=4{,}3\cdot(\lg\mathrm{Re})^{-2},\qquad \mathrm{Re}>700;$$
$$\mathrm{Re}=\frac{\rho_1^{tm}\cdot|u_1-u_2|\cdot d_p}{\mu_1}.$$

The expressions for c_x and c_r have the similar structure of record.

The expression for the function of thermal interphase interaction caused by compelled convection is defined by the formula:

$$q=n\cdot\pi\cdot d_p\cdot\lambda_1\cdot Nu\cdot(T_1-T_2),\tag{9}$$

where

$$Nu = 2 + 0{,}6 \cdot \mathrm{Re}^{0,5} \cdot \mathrm{Pr}^{0,333};$$

$$\mathrm{Re} = \frac{\rho_1^{tm} \cdot |\mathbf{W}_1 - \mathbf{W}_2| \cdot d_p}{\mu_1}; \quad \mathrm{Pr} = \frac{c_p \cdot \mu_1}{\lambda_1}.$$

The system of the equations (1) - (3) is integrated numerically by means of the Davydov's method [12-15 etc.]. Within the framework of the considered task we will name all stages of the computing cycle of the method separately. The area of integration consist of the fixed in space (Eulerian), uniform orthogonal grid with cells $\Delta x \times \Delta r$. The meanings of integers "i" (along the axis 0X) and "j" (along the axis 0R) designate the centre of a cell. On irregular (not conterminous with the grid) borders of the settlement area the device of fractional cells is applied [17]. The settlement formulas only for the whole cells everywhere are used.

Eulerian stage. At this stage the units change concerning a cell as a whole and the investigated media (heterogeneous mix of gas and firm particles) is assumed as frozen. Therefore convecting members of the kind $div\,(\rho_i \varphi \mathbf{W}_i)$,where $\varphi = (1, u_i, v_i, J_2, E_i)$, $i = (1,2)$, appropriate to moving effects, in the system (1) - (3) are rejected. Besides, obtained complexes and both power and thermal interphase interaction included in the right-hand sides of the equations, become zero. The equations of indissolubility (1), in particular, are simplified. Therefore it is possible to distinguish the rest of equations of the system ρ_i and solve (1) - (3) concerning temporary derivatives from u_i, v_i, E_1.

Then we have:

$$\rho_1 \cdot \frac{\partial u_1}{\partial t} + \alpha \cdot \frac{\partial p}{\partial x} = 0;$$

$$\rho_1 \cdot \frac{\partial v_1}{\partial t} + \alpha \cdot \frac{\partial p}{\partial r} = 0;$$

$$\rho_2 \cdot \frac{\partial u_2}{\partial t} + (1-\alpha) \cdot \frac{\partial p}{\partial x} = 0;$$

$$\rho_2 \cdot \frac{\partial v_2}{\partial t} + (1-\alpha) \cdot \frac{\partial p}{\partial r} = 0; \tag{10}$$

$$E_2 = J_2 + \frac{u_2^2 + v_2^2}{2};$$

$$\rho_1 \cdot \frac{\partial E_1}{\partial t} + \rho_2 \cdot \frac{\partial E_2}{\partial t} + div(\alpha p \mathbf{W}_1) + div[(1-\alpha) p \mathbf{W}_2] = 0.$$

We approximate, at the moment time t^n, the equation of system (10) by the obvious parametrical finite-difference scheme. Finding (10) the required units, we will receive the following margin of the equation of the first order of accuracy in time and of the second order of accuracy in space for a cell (large particle) "i, j":

$$\tilde{u}^n_{1_{i,j}} = u^n_{1_{i,j}} - \alpha^n_{i,j} \cdot \frac{p^n_{i+0.5,j} - p^n_{i-0.5,j}}{\Delta x} \cdot \frac{\Delta t}{\rho^n_{1_{i,j}}};$$

$$\tilde{v}^n_{1_{i,j}} = v^n_{1_{i,j}} - \alpha^n_{i,j} \cdot \frac{p^n_{i,j+0.5} - p^n_{i,j-0.5}}{\Delta r} \cdot \frac{\Delta t}{\rho^n_{1_{i,j}}};$$

$$\tilde{u}^n_{2_{i,j}} = u^n_{2_{i,j}} - (1 - \alpha^n_{i,j}) \cdot \frac{p^n_{i+0.5,j} - p^n_{i-0.5,j}}{\Delta x} \cdot \frac{\Delta t}{\rho^n_{2_{i,j}}};$$

$$\tilde{v}^n_{2_{i,j}} = v^n_{2_{i,j}} - (1 - \alpha^n_{i,j}) \cdot \frac{p^n_{i,j+0.5} - p^n_{i,j-0.5}}{\Delta r} \cdot \frac{\Delta t}{\rho^n_{2_{i,j}}};$$

$$\tilde{E}^n_{2_{i,j}} = J^n_{2_{i,j}} + \frac{\left(\tilde{u}^n_{2_{i,j}}\right)^2 + \left(\tilde{v}^n_{2_{i,j}}\right)^2}{2};$$

$$\tilde{E}^n_{1_{i,j}} = E^n_{1_{i,j}} - \left(\tilde{E}^n_{2_{i,j}} - E^n_{2_{i,j}}\right) \cdot \frac{\rho^n_{2_{i,j}}}{\rho^n_{1_{i,j}}} - \tag{11}$$

$$\frac{\alpha^n_{i+0.5,j} \cdot p^n_{i+0.5,j} \cdot \bar{u}^n_{1_{i+0.5,j}} - \alpha^n_{i-0.5,j} \cdot p^n_{i-0.5,j} \cdot \bar{u}^n_{1_{i-0.5,j}}}{\Delta x} \cdot \frac{\Delta t}{\rho^n_{1_{i,j}}} -$$

$$\frac{j \cdot \alpha^n_{i,j+0.5} \cdot p^n_{i,j+0.5} \cdot \bar{v}^n_{1_{i,j+0.5}} - (j-1) \cdot \alpha^n_{i,j-0.5} \cdot p^n_{i,j-0.5} \cdot \bar{v}^n_{1_{i,j-0.5}}}{(j-0{,}5) \cdot \Delta r} \cdot \frac{\Delta t}{\rho^n_{1_{i,j}}} -$$

$$\frac{(1-\alpha^n_{i+0.5,j}) \cdot p^n_{i+0.5,j} \cdot u^n_{2_{i+0.5,j}} - (1-\alpha^n_{i-0.5,j}) \cdot p^n_{i-0.5,j} \cdot u^n_{2_{i-0.5,j}}}{\Delta x} \cdot \frac{\Delta t}{\rho^n_{1_{i,j}}} -$$

$$\frac{j \cdot (1-\alpha^n_{i,j+0.5}) \cdot p^n_{i,j+0.5} \cdot v^n_{2_{i,j+0.5}} - (j-1) \cdot (1-\alpha^n_{i,j-0.5}) \cdot p^n_{i,j-0.5} \cdot v^n_{2_{i,j-0.5}}}{(j-0{,}5) \cdot \Delta r} \cdot \frac{\Delta t}{\rho^n_{1_{i,j}}}.$$

In (11) the following designations are accepted:

$$p^n_{i+0.5,j} = \frac{p^n_{i,j} + p^n_{i+1,j}}{2};$$
$$\bar{u}^n_{1_{i,j}} = (1 - alfa)\cdot u^n_{1_{i,j}} + alfa \cdot \tilde{u}^n_{1_{i,j}};$$
$$\bar{v}^n_{1_{i,j}} = (1 - alfa)\cdot v^n_{1_{i,j}} + alfa \cdot \tilde{v}^n_{1_{i,j}},$$

where $alfa$ - grid parameter, which value can change within the limits $alfa = (0{,}0 - 8{,}0)$.

In certain cases for the calculation of stability increase of the Eulerian stage of the Davydov's method (particularly in settlement zones with fairly constant pressure, by small speeds of movement of a flow and large speed of a sound ~ $M < 0{,}1$) it is expedient to use implicit finite-difference schemes.

Lagrangian stage. At the given stage of the method the effects of transference, which is taking into the account an exchange among cells at their reorganization on the former Eulerian grid, are calculated. Here in time Δt there are flows of mass, pulse and energy through borders of Eulerian cells for each phase of a heterogeneous mix.

Flow-line formulas can be written down differently. The choice of the record form of these units has the important meaning, as it strongly influences stability and accuracy of the simulation. In the given version of the Lagrangian stage we will define flows of mass, pulse and energy by the following parametrical formulas of the first order of accuracy:

- the first phase along the axis 0X

$$(\rho_1 \varphi \tilde{u}_1)^n_{i+0.5,j} = \begin{cases} \left[(1 - beta)\cdot \rho^n_{1_{i,j}} + beta \cdot \rho^n_{1_{i+1,j}}\right]\cdot \varphi^n_{i,j} \cdot \tilde{u}^n_{1_{i+0.5,j}}, & \text{if } \tilde{u}^n_{1_{i+0.5,j}} \ge 0; \\ \left[(1 - beta)\cdot \rho^n_{1_{i+1,j}} + beta \cdot \rho^n_{1_{i,j}}\right]\cdot \varphi^n_{i+1,j} \cdot \tilde{u}^n_{1_{i+0.5,j}}, & \text{if } \tilde{u}^n_{1_{i+0.5,j}} < 0; \end{cases}$$
$$\varphi = \left(1, \tilde{u}_1, \tilde{v}_1, \tilde{E}_1\right); \tag{12}$$

- the first phase along the axis 0R

$$(\rho_1 \varphi \tilde{v}_1)^n_{i,j+0.5} = \begin{cases} \left[(1 - beta)\cdot \rho^n_{1_{i,j}} + beta \cdot \rho^n_{1_{i,j+1}}\right]\cdot \varphi^n_{i,j} \cdot \tilde{v}^n_{1_{i,j+0.5}}, & \text{if } \tilde{v}^n_{1_{i,j+0.5}} \ge 0; \\ \left[(1 - beta)\cdot \rho^n_{1_{i,j+1}} + beta \cdot \rho^n_{1_{i,j}}\right]\cdot \varphi^n_{i,j+1} \cdot \tilde{v}^n_{1_{i,j+0.5}}, & \text{if } \tilde{v}^n_{1_{i,j+0.5}} < 0; \end{cases}$$
$$\varphi = \left(1, \tilde{u}_1, \tilde{v}_1, \tilde{E}_1\right); \tag{13}$$

- the second phase along the axis 0X

$$(\rho_2 \varphi \tilde{u}_2)^n_{i+0.5,j} = \begin{cases} \rho^n_{2_{i,j}} \cdot \varphi^n_{i,j} \cdot \tilde{u}^n_{2_{i+0.5,j}}, \text{ если } \tilde{u}^n_{2_{i+0.5,j}} \ge 0; \\ \rho^n_{2_{i+1,j}} \cdot \varphi^n_{i+1,j} \cdot \tilde{u}^n_{2_{i+0.5,j}}, \text{ если } \tilde{u}^n_{2_{i+0.5,j}} < 0; \end{cases}$$
$$\varphi = \left(1, \tilde{u}_2, \tilde{v}_2, J_2, \tilde{E}_2\right); \tag{14}$$

- the second phase along the axis 0R

$$(\rho_2 \varphi \tilde{v}_2)^n_{i,j+0.5} = \begin{cases} \rho^n_{2_{i,j}} \cdot \varphi^n_{i,j} \cdot \tilde{v}^n_{2_{i,j+0.5}}, \text{ если } \tilde{v}^n_{2_{i,j+0.5}} \ge 0; \\ \rho^n_{2_{i,j+1}} \cdot \varphi^n_{i,j+1} \cdot \tilde{v}^n_{2_{i,j+0.5}}, \text{ если } \tilde{v}^n_{2_{i,j+0.5}} < 0; \end{cases}$$
$$\varphi = \left(1, \tilde{u}_2, \tilde{v}_2, J_2, \tilde{E}_2\right). \tag{15}$$

In expressions (12) - (15) $beta$ - grid parameter, which value can change within the limits: $beta = (-0{,}3 - 0{,}0)$.

On the Lagrangian stage of the method obtained complexes and both force and thermal functions interphase interaction (5) - (9) included in right-hand sides of the equations (1) - (3) are also calculated, in view of change of a flow parameters in Eulerian stage.

Final stage. Here occurs a redistribution of mass, pulse and energy in space and the final fields of the Eulerian parameters of a biphase heterogeneous flow on the fixed grid are determined at the moment of time. The equations of this stage represent the laws of preservation of mass, pulse and energy, which have been written down in view of intermediate values of the flow parameters and presence of obtained complexes and functions of interphase interaction that are determined in Eulerian and Lagrangian stages.

The initial system of the differential equations (1) - (3) looks as:

- the equations of indissolubility (preservation of mass)

$$\frac{\partial \rho_1}{\partial t} + div\left(\rho_1 \tilde{\mathbf{W}}_1\right) = G_{gw};$$
$$\frac{\partial \rho_2}{\partial t} + div\left(\rho_2 \tilde{\mathbf{W}}_2\right) = G_{pw}; \qquad (16)$$

- the equations of a pulse preservation on axes of coordinates

$$\frac{\partial\left(\rho_1 \tilde{u}_1\right)}{\partial t} + div\left(\rho_1 \tilde{u}_1 \tilde{\mathbf{W}}_1\right) = -\tau_x + W_x \cdot G_{gw};$$
$$\frac{\partial\left(\rho_1 \tilde{v}_1\right)}{\partial t} + div\left(\rho_1 \tilde{v}_1 \tilde{\mathbf{W}}_1\right) = -\tau_r + W_r \cdot G_{gw};$$
$$\frac{\partial\left(\rho_2 \tilde{u}_2\right)}{\partial t} + div\left(\rho_2 \tilde{u}_2 \tilde{\mathbf{W}}_2\right) = \tau_x + W_x \cdot G_{pw}; \qquad (17)$$
$$\frac{\partial\left(\rho_2 \tilde{v}_2\right)}{\partial t} + div\left(\rho_2 \tilde{v}_2 \tilde{\mathbf{W}}_2\right) = \tau_r + W_r \cdot G_{pw};$$

- the equations of specific energy preservation
-

$$\frac{\partial\left(\rho_2 J_2\right)}{\partial t} + div\left(\rho_2 J_2 \tilde{\mathbf{W}}_2\right) = q + J_{pw} \cdot G_{pw};$$
$$\frac{\partial\left(\rho_1 \tilde{E}_1\right)}{\partial t} + \frac{\partial\left(\rho_2 \tilde{E}_2\right)}{\partial t} + div\left(\rho_1 \tilde{E}_1 \tilde{\mathbf{W}}_1\right) + div\left(\rho_2 \tilde{E}_2 \tilde{\mathbf{W}}_2\right) = \qquad (18)$$
$$J_{gw} \cdot G_{gw} + J_{pw} \cdot G_{pw},$$

where for axi-symmetric case

$$div\left(\varphi \tilde{\mathbf{W}}_i\right) = \frac{\partial\left(\varphi \tilde{u}_i\right)}{\partial x} + \frac{1}{r} \cdot \frac{\partial\left(r \varphi \tilde{v}_i\right)}{\partial r},$$

$$\varphi = \left(\rho_i, \rho_i \tilde{u}_i, \rho_i \tilde{v}_i, \rho_2 J_2, \rho_i \tilde{E}_i\right);$$
$$i = (1,2).$$

We approximate the equation (16) - (18) on a new temporary layer $t^{n+1} = t^n + \Delta t$ and solving them concerning required units, we will receive the following obvious finite-difference parities for "i, j" cells (large particle):

- the equations of indissolubility (preservation of mass)

$$\rho_{1_{i,j}}^{n+1} = \rho_{1_{i,j}}^{n} - \frac{\left(\rho_1 \tilde{u}_1\right)_{i+0.5,j}^{n} - \left(\rho_1 \tilde{u}_1\right)_{i-0.5,j}^{n}}{\Delta x} \cdot \Delta t - \frac{j \cdot \left(\rho_1 \tilde{v}_1\right)_{i,j+0.5}^{n} - (j-1) \cdot \left(\rho_1 \tilde{v}_1\right)_{i,j-0.5}^{n}}{(j-0{,}5) \cdot \Delta r} \cdot \Delta t + G_{gw_{i,j}}^{n} \cdot \Delta t;$$

$$\rho_{2_{i,j}}^{n+1} = \rho_{2_{i,j}}^{n} - \frac{\left(\rho_2 \tilde{u}_2\right)_{i+0.5,j}^{n} - \left(\rho_2 \tilde{u}_2\right)_{i-0.5,j}^{n}}{\Delta x} \cdot \Delta t - \frac{j \cdot \left(\rho_2 \tilde{v}_2\right)_{i,j+0.5}^{n} - (j-1) \cdot \left(\rho_2 \tilde{v}_2\right)_{i,j-0.5}^{n}}{(j-0{,}5) \cdot \Delta r} \cdot \Delta t + G_{pw_{i,j}}^{n} \cdot \Delta t;$$

- the equations of a pulse preservation

$$u_{1_{i,j}}^{n+1} = \tilde{u}_{1_{i,j}}^{n} \cdot \frac{\rho_{1_{i,j}}^{n}}{\rho_{1_{i,j}}^{n+1}} - \frac{\left(\rho_1 \tilde{u}_1 \tilde{u}_1\right)_{i+0.5,j}^{n} - \left(\rho_1 \tilde{u}_1 \tilde{u}_1\right)_{i-0.5,j}^{n}}{\Delta x} \cdot \frac{\Delta t}{\rho_{1_{i,j}}^{n+1}} - \frac{j \cdot \left(\rho_1 \tilde{u}_1 \tilde{v}_1\right)_{i,j+0.5}^{n} - (j-1) \cdot \left(\rho_1 \tilde{u}_1 \tilde{v}_1\right)_{i,j-0.5}^{n}}{(j-0{,}5) \cdot \Delta r} \cdot \frac{\Delta t}{\rho_{1_{i,j}}^{n+1}} - \tau_{x_{i,j}}^{n} \cdot \frac{\Delta t}{\rho_{1_{i,j}}^{n+1}} + W_{x_{i,j}}^{n} \cdot G_{gw_{i,j}}^{n} \cdot \frac{\Delta t}{\rho_{1_{i,j}}^{n+1}};$$

$$v_{1_{i,j}}^{n+1} = \tilde{v}_{1_{i,j}}^{n} \cdot \frac{\rho_{1_{i,j}}^{n}}{\rho_{1_{i,j}}^{n+1}} - \frac{\left(\rho_1 \tilde{v}_1 \tilde{u}_1\right)_{i+0.5,j}^{n} - \left(\rho_1 \tilde{v}_1 \tilde{u}_1\right)_{i-0.5,j}^{n}}{\Delta x} \cdot \frac{\Delta t}{\rho_{1_{i,j}}^{n+1}} - \frac{j \cdot \left(\rho_1 \tilde{v}_1 \tilde{v}_1\right)_{i,j+0.5}^{n} - (j-1) \cdot \left(\rho_1 \tilde{v}_1 \tilde{v}_1\right)_{i,j-0.5}^{n}}{(j-0{,}5) \cdot \Delta r} \cdot \frac{\Delta t}{\rho_{1_{i,j}}^{n+1}} - \tau_{r_{i,j}}^{n} \cdot \frac{\Delta t}{\rho_{1_{i,j}}^{n+1}} + W_{r_{i,j}}^{n} \cdot G_{gw_{i,j}}^{n} \cdot \frac{\Delta t}{\rho_{1_{i,j}}^{n+1}}; \qquad (20)$$

$$u_{2_{i,j}}^{n+1} = \tilde{u}_{2_{i,j}}^{n} \cdot \frac{\rho_{2_{i,j}}^{n}}{\rho_{2_{i,j}}^{n+1}} - \frac{\left(\rho_2 \tilde{u}_2 \tilde{u}_2\right)_{i+0.5,j}^{n} - \left(\rho_2 \tilde{u}_2 \tilde{u}_2\right)_{i-0.5,j}^{n}}{\Delta x} \cdot \frac{\Delta t}{\rho_{2_{i,j}}^{n+1}} - \frac{j \cdot \left(\rho_2 \tilde{u}_2 \tilde{v}_2\right)_{i,j+0.5}^{n} - (j-1) \cdot \left(\rho_2 \tilde{u}_2 \tilde{v}_2\right)_{i,j-0.5}^{n}}{(j-0{,}5) \cdot \Delta r} \cdot \frac{\Delta t}{\rho_{2_{i,j}}^{n+1}} + \tau_{x_{i,j}}^{n} \cdot \frac{\Delta t}{\rho_{2_{i,j}}^{n+1}} + W_{x_{i,j}}^{n} \cdot G_{pw_{i,j}}^{n} \cdot \frac{\Delta t}{\rho_{2_{i,j}}^{n+1}};$$

$$v_{2_{i,j}}^{n+1} = \tilde{v}_{2_{i,j}}^{n} \cdot \frac{\rho_{2_{i,j}}^{n}}{\rho_{2_{i,j}}^{n+1}} - \frac{\left(\rho_2 \tilde{v}_2 \tilde{u}_2\right)_{i+0.5,j}^{n} - \left(\rho_2 \tilde{v}_2 \tilde{u}_2\right)_{i-0.5,j}^{n}}{\Delta x} \cdot \frac{\Delta t}{\rho_{2_{i,j}}^{n+1}} - \frac{j \cdot \left(\rho_2 \tilde{v}_2 \tilde{v}_2\right)_{i,j+0.5}^{n} - (j-1) \cdot \left(\rho_2 \tilde{v}_2 \tilde{v}_2\right)_{i,j-0.5}^{n}}{(j-0{,}5) \cdot \Delta r} \cdot \frac{\Delta t}{\rho_{2_{i,j}}^{n+1}} + \tau_{r_{i,j}}^{n} \cdot \frac{\Delta t}{\rho_{2_{i,j}}^{n+1}} + W_{r_{i,j}}^{n} \cdot G_{pw_{i,j}}^{n} \cdot \frac{\Delta t}{\rho_{2_{i,j}}^{n+1}};$$

- the equations of specific energy preservation

$$J_{2_{i,j}}^{n+1} = J_{2_{i,j}}^{n} \cdot \frac{\rho_{2_{i,j}}^{n}}{\rho_{2_{i,j}}^{n+1}} - \frac{(\rho_2 J_2 \tilde{u}_2)_{i+0.5,j}^{n} - (\rho_2 J_2 \tilde{u}_2)_{i-0.5,j}^{n}}{\Delta x} \cdot \frac{\Delta t}{\rho_{2_{i,j}}^{n+1}} - \frac{j \cdot (\rho_2 J_2 \tilde{v}_2)_{i,j+0.5}^{n} - (j-1) \cdot (\rho_2 J_2 \tilde{v}_2)_{i,j-0.5}^{n}}{(j-0,5) \cdot \Delta r} \cdot \frac{\Delta t}{\rho_{2_{i,j}}^{n+1}} + \left(q_{i,j}^{n} + J_{pw_{i,j}}^{n} \cdot G_{pw_{i,j}}^{n}\right) \cdot \frac{\Delta t}{\rho_{2_{i,j}}^{n+1}};$$

$$E_{2_{i,j}}^{n+1} = J_{2_{i,j}}^{n+1} + \frac{\left(u_{2_{i,j}}^{n+1}\right)^2 + \left(v_{2_{i,j}}^{n+1}\right)^2}{2}; \qquad (21)$$

$$E_{1_{i,j}}^{n+1} = \tilde{E}_{1_{i,j}}^{n} \cdot \frac{\rho_{1_{i,j}}^{n}}{\rho_{1_{i,j}}^{n+1}} - \frac{\rho_{2_{i,j}}^{n+1} \cdot E_{2_{i,j}}^{n+1} - \rho_{2_{i,j}}^{n} \cdot \tilde{E}_{2_{i,j}}^{n}}{\rho_{1_{i,j}}^{n+1}} - \frac{\left(\rho_1 \tilde{E}_1 \tilde{u}_1\right)_{i+0.5,j}^{n} - \left(\rho_1 \tilde{E}_1 \tilde{u}_1\right)_{i-0.5,j}^{n}}{\Delta x} \cdot \frac{\Delta t}{\rho_{1_{i,j}}^{n+1}} - \frac{j \cdot \left(\rho_1 \tilde{E}_1 \tilde{v}_1\right)_{i,j+0.5}^{n} - (j-1) \cdot \left(\rho_1 \tilde{E}_1 \tilde{v}_1\right)_{i,j-0.5}^{n}}{(j-0,5) \cdot \Delta r} \cdot \frac{\Delta t}{\rho_{1_{i,j}}^{n+1}} - \frac{\left(\rho_2 \tilde{E}_2 \tilde{u}_2\right)_{i+0.5,j}^{n} - \left(\rho_2 \tilde{E}_2 \tilde{u}_2\right)_{i-0.5,j}^{n}}{\Delta x} \cdot \frac{\Delta t}{\rho_{1_{i,j}}^{n+1}} - \frac{j \cdot \left(\rho_2 \tilde{E}_2 \tilde{v}_2\right)_{i,j+0.5}^{n} - (j-1) \cdot \left(\rho_2 \tilde{E}_2 \tilde{v}_2\right)_{i,j-0.5}^{n}}{(j-0,5) \cdot \Delta r} \cdot \frac{\Delta t}{\rho_{1_{i,j}}^{n+1}} + \left(J_{gw_{i,j}}^{n} \cdot G_{gw_{i,j}}^{n} + J_{pw_{i,j}}^{n} \cdot G_{pw_{i,j}}^{n}\right) \cdot \frac{\Delta t}{\rho_{1_{i,j}}^{n+1}}.$$

Algorithmically the parameters of the second phase - phase of particles (toted phase) are calculated at first following by the parameters of the first - gas phase (transferring phase). Subsequently the pressure of combustion products is calculated by means of recalculation in the equation of condition (4).

For increase of calculation accuracy in the scheme of the method at simulation of pressure an additional amendment ensuring balance on internal specific energy of the gas phase is inserted. Thus, for the gas phase of a heterogeneous mix condition of complete conservatism of finite-difference circuits of a method is satisfied. Expression for calculation of pressure has the following form:

$$p_{i,j}^{n+1} = (k-1) \cdot \left(\rho_1^{u}\right)_{i,j}^{n+1} \cdot \left\{E_{1_{i,j}}^{n+1} - \frac{1}{2} \cdot \left[\left(W_{1_{i,j}}^{n+1}\right)^2 + \frac{\rho_{1_{i,j}}^{n}}{\rho_{1_{i,j}}^{n+1}} \cdot \left(\Delta W_{1_{i,j}}^{*}\right)^2\right]\right\}, \qquad (22)$$

where

$$\left(W_{1_{i,j}}^{n+1}\right)^2 = \left(u_{1_{i,j}}^{n+1}\right)^2 + \left(v_{1_{i,j}}^{n+1}\right)^2,$$

$$\left(\Delta W_{1_{i,j}}^{*}\right)^2 = \left(u_{1_{i,j}}^{n+1} - \tilde{u}_{1_{i,j}}^{n}\right)^2 + \left(v_{1_{i,j}}^{n+1} - \tilde{v}_{1_{i,j}}^{n}\right)^2.$$

At this point the performance of the third (final) stage, the computing cycle of the Davydov's method approaches the end.

Let's make an important remark on statement of the boundary conditions. At numerical modeling of the low-frequency acoustic instability in the solid propellant rocket engine it is necessary to provide that perturbations are generated by the flow of combustion products remained in settlement area (combustion chamber) and didn't leave through open borders. For this reason at the statement of boundary conditions of the walls of the combustion chamber of the engine, the burning surface of a solid propellant charge and the nozzle walls should be considered as impenetrable border for perturbation.

Let's look at some results of simulations.

Fig. 1 presents the basic layout circuit of free volume of the combustion chamber of SPRE on variant 1 and the change in time (within the framework of the several fluctuation periods) of pressure (in deviation from the average meaning at the given point) in the combustion chamber. The pressure is presented in the area of the forward bottom of the engine (position À). The amplitude of pressure fluctuations is $A_p = 0{,}55$ MPa. Frequency of pressure fluctuations - $f = 77$ Hz. The process of fluctuations is steady.

Fig. 2 provides the basic layout circuit of free volume of the combustion chamber of SPRE on variant 2 and temporal change of pressure in the combustion chamber. The presented parameters are analogous to the data in the Fig. 1. The amplitude of pressure fluctuations is $A_p = 0{,}21$ MPa. Frequency of pressure fluctuations is $f = 76$ Hz. The process of fluctuations is steady.

On the basis of the given data it is possible to make a conclusion about the essential influence of the geometrical form of the combustion chamber on magnitude of the pressure fluctuations amplitude in SPRE. At the right choice of the configuration of the combustion chamber the amplitude of pressure fluctuations decreases by *0,55/0,21 = 2,62* times! Thus the frequency of pressure fluctuations in the combustion chamber of the engine varies insignificantly.

Let's consider in detail the dynamic case of the distribution of gas-dynamic parameters of the current in free volume of the combustion chamber of SPRE up to an entrance of a flow in the nozzle. The layout circuit of free volume of the combustion chamber of the engine is presented in a Fig. 1. Let's compare the parameters of the flow of combustion products at the various moments of time (within the framework of one period of pressure fluctuations) along the length of the combustion chamber in the following conic-cylindrical sections (Fig. 1): at the axis of symmetry and at the burning surface of a solid propellant charge and wall of the combustion chamber (ABCD).

Fig. 3 illustrates the distribution of the horizontal projection of movement speed of gas combustion products u_1 on length of the combustion chamber of SPRE in two fixed conic-cylindrical sections at the various moments of time. The distribution of the vertical projection of movement speed of gas combustion products practically is homogeneous and essentially does not vary in time. The exception is made only with the local zone in the area of the rocket engine nozzle, which is not considered here.

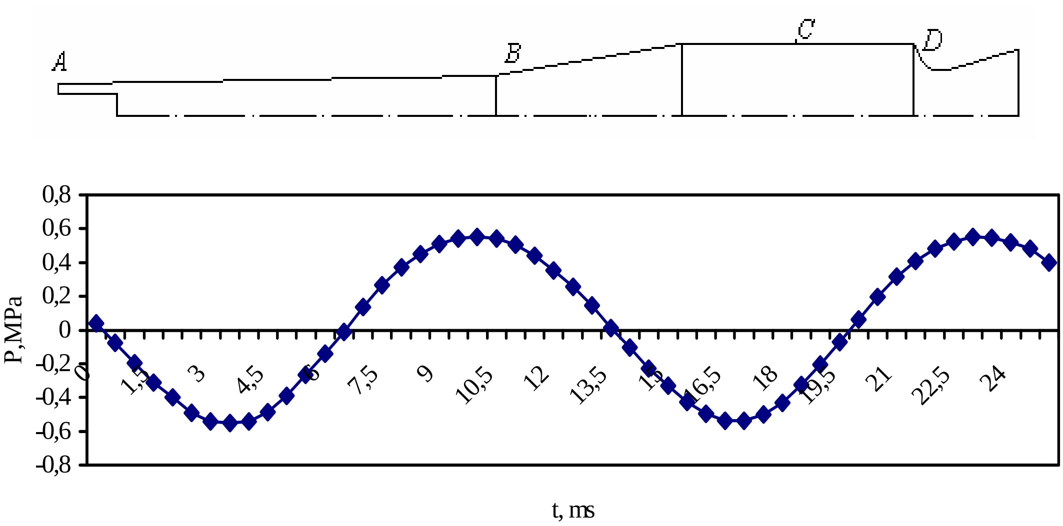

Fig. 1. Layout circuit of the combustion chamber of SPRE on variant 1 and change in time of pressure in the combustion chamber

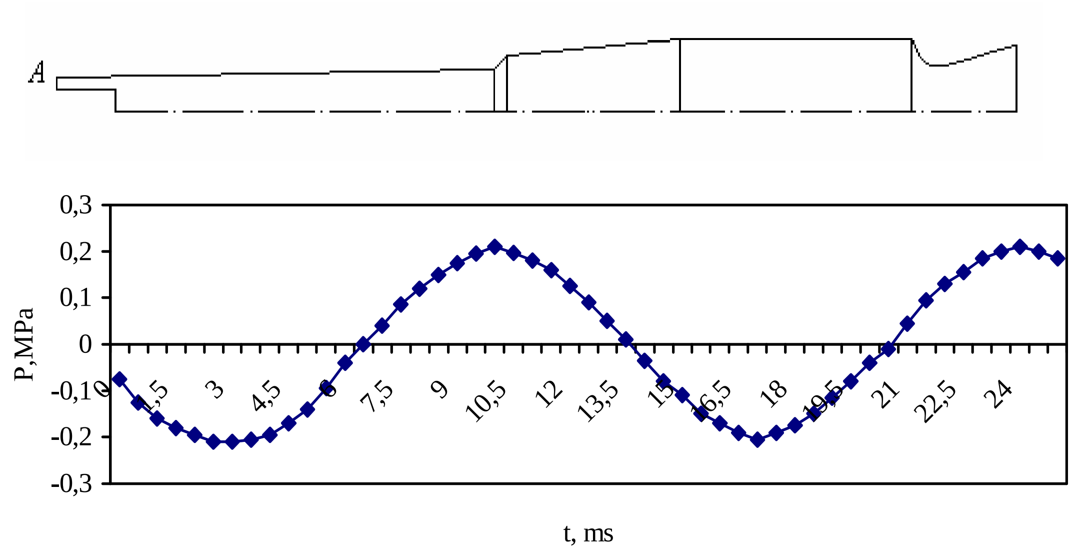

Fig. 2. Layout circuit of the combustion chamber of SPRE on variant 2 and change in time of pressure in the combustion chamber

At the moment of time $t = 2{,}5$ ms (Fig. 3) along the symmetry axis from the forward bottom (position A, see Fig. 1) up to the beginning of the large opposite obliquity area (position B) increase of combustion products movement speed up to $u_{1\max} \approx 182$ m/s occurs. At deeper input in area of large opposite obliquity, the flow slightly slows down. And further, getting into the nozzle, is intensively accelerated. At the given moment in time the essential change on the radius of the combustion chamber of the horizontal projection of the movement speed of gas combustion products is observed, and this change is the most appreciable at the burning surface of a solid propellant charge (surface ABC, see Fig. 1) and at the lateral wall of the combustion chamber (surface CD, see Fig. 1). In the background of the general direction of movement of flow of combustion products from the forward bottom to the nozzle is observed precisely

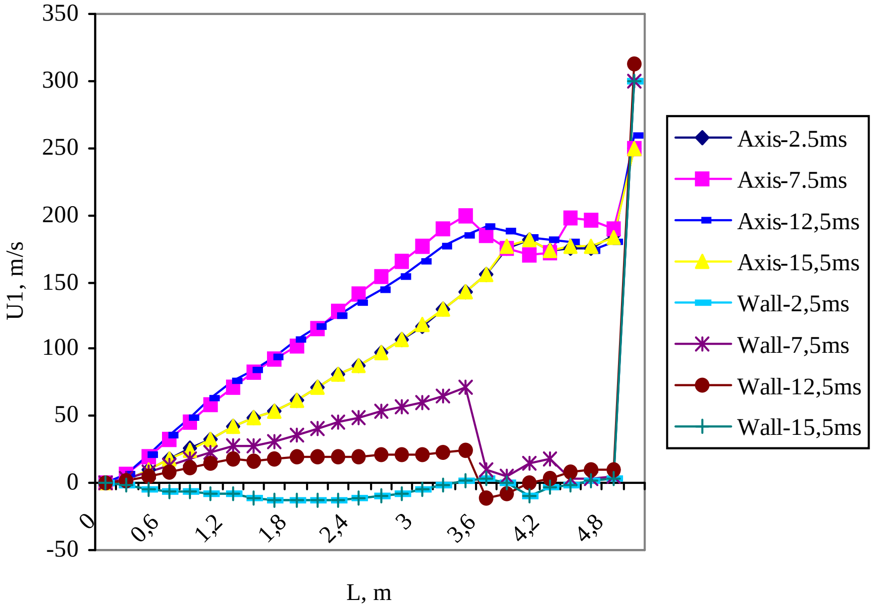

Fig. 3. Distribution of longitudinal making movement speed of combustion products on length of the combustion chamber of SPRE at the various moments of time (layout circuit of the combustion chamber on variant 1)

expressed counter-flow at the burning surface of a solid propellant charge. Combustion products move here from the nozzle to the forward bottom. The horizontal projection of the speed component of counter-flow reaches the value of $u_{1\max} \approx 182$ m/s. In the back bottom area at the wall of the combustion chamber (position D, see Fig. 1) the extensive zone of the slow-down of flow of combustion products is formed.

At the moment of time $t = 7{,}5$ ms (Fig. 3) along the axis of symmetry from the forward bottom up to the beginning of the area of the large opposite obliquity the increase of movement speed of combustion products up to $u_{1\max} \approx 199$ m/s is observed. At the entrance in the area of the large opposite obliquity and further in the area of the back bottom the flow slows down a little. Getting in the nozzle, the combustion products flow is intensively accelerated. At the given moment in time the change on the radius of the combustion chamber of the horizontal projection of the movement speed of combustion products is also observed. However the zone of the counter-flow along the burning surface of a solid propellant charge is not present here. The longitudinal component of speed of combustion products flow along the burning surface from the forward bottom in the nozzle direction is increased gradually and reaches the value of $u_{1\max} \approx 72$ m/s. Further at an input of parietal flow in the area of the large opposite obliquity its speed greatly decreases up to $u_{1\min} \approx 5$ m/s. In the area of the back bottom at the combustion chamber wall the extensive zone of slow-down of flow of the combustion products is maintained.

At the moment in time $t = 12{,}5$ m/s (Fig. 3) in the background of general direction of a combustion products flow movement from the forward bottom to the nozzle at the burning surface of a solid propellant charge in the area of the forward bottom and in the area of the large opposite obliquity start to arise local zones of counter-flow. The size of horizontal projection of the speed of movement of the combustion products flow along the burning surface of a charge decreases to $u_{1\max} \approx 24$ m/s and $u_{1\min} \approx -12$ m/s. The conditions for formation of extensive area of return current along a solid propellant burning surface are gradually prepared.

Further from the moment in time $t = 15{,}5$ ms (Fig. 3), at the period of pressure fluctuations $\tau \approx 13$ ms, the picture of current in the combustion chamber of SPRE begins to repeat cyclically (line "Axis - 2,5 ms" and "Axis - 15,5 ms", "Wall - 2,5 ms" and "Wall - 15,5 ms" practically coincide).

Thus, it is necessary to find the reasons for generation (excitation and refill) of oscillatory process in the structure and the character of the combustion products current in the combustion chamber of SPRE. The fluctuations here have hydro-dynamical highly nonlinear nature. Frequency and amplitude of fluctuations (amplitude in particular) depend on a number of factors. The main of them are: the presence of essential stratification of the flow of combustion products along the radius of the combustion chamber according to the parameters (mainly of speed) of the current. The flow of such complex structure at the entrance into the nozzle irregularly cooperates with the wall of the back bottom of the engine and is partially reflected from it. In the area of the back bottom at the lateral wall of the combustion chamber the opposite flow is formed or the flow essentially slows down. Thus, non-stationary low-frequency acoustic pulsing current in the combustion chamber of SPRE is raised and subsequently (due to the finite size of the combustion chamber) is cyclically refilled.

References

1. **Ragulskis K. M., Bastytė L., Astrauskienė E., Ragulskis M**. The dynamics and stability of subharmonic motion of mechanisms on a vibration basis as essentially nonlinear systems. - In: Wave mechanical systems, Proceedings of international seminar. - Kaunas, Lithuanian Academy of Sciences, Kaunas University of Technology, 1994, p. 80-83.
2. **Ragulskis K. M., Vitkus J., Ragulskienė V.** Selfsynchronization of mechanical systems (1. Self-synchronous and vibroshock systems). – Vilnus: Minis, 1965. – 187 p. (in Russian).
3. Solid Propellant Rocket Research. / Editor by M. Summerfield. – New York – London: Academic Press, 1960. – 440 p.
4. **Kolesnikov K. S.** Longitudinal fluctuations of a rocket with the liquid rocket engine. – M.: Mashinostroenie, 1971. - 260 p. (Russian).
5. **Melkumov T. M., Melik-Pashaev N. I., Chistiakov P. G., Shiutov A. G.** Rocket Engine. – M.: Mashinostoenie, 1976. – 400 p. (Russian).
6. **Alemasov B. E., Dregalin A. F., Tishin A. P.** The Theory of Rocket Engines. – M.: Mashinostoenie, 1980. – 533 p. (Russian).
7. Blohintsev D. I. Acoustics of Non-uniform Driven Environment. – M.: Nauka, 1981. – 206 p. (Russian).
8. **Suhinin S. B., Ahmadeev B. F.** Hydrodynamical Sources of Fluctuations in Chambers of Combustion. - Physics of burning and explosion, 1993, vol.29, №6, p.38-46 (Russian).
9. **Vaganova N. A., Kovrijnyh O. O., Kokovihina O. B., Sidorov A. F., Hairulina O. B.** Gas-dynamic and Acoustic Effects in Chambers of Combustion of Rocket Engines of Firm Fuel. – In: All-Russia Scientific-Practical Conference “The First Ocunev Readings”. / In 2 Volumes. Volume 1. Ballistics. – Saint-Petersburg: BSTU, 1999, p. 118–129 (Russian).
10. **Davydov Yu. M., Egorov M. Yu.** Numerical Modelling of Nonstationary Transitional Processes in Active and Reactive Engines. – M.: NAAS RF, 1999. – 272 p. (Russian).
11. **Davydov Yu. M., Egorov M. Yu.** The Instability of the Working Process in the Combustion Chamber of a Solid-Propellant Rocket Engine. – Doklady Physics, 2001, number 3, vol. 46, p. 195.
12. **Davydov Yu. M., Davydova In. M., Egorov M. Yu.** Inprovement And Optimization of Aircraft And Rocket Engines With Taking Into Consideration Nonlinear Non-stationary Gas-Dynamics Effects. - M.: NAAS RF, 2002. – 303 p. (Russian).
13. **Davydov Yu. M.** Large-particle method. - In: Mathematical encyclopedia. Vol.3. – M.: Soviet encyclopedia, 1982, p.125-129. (Russian).
14. **Davydov Yu. M.** Large-particle method. - In: Encyclopaedia of mathematics, vol. 5. – Dordrecht / Boston / London: Kluver academic publishers, 1990, p. 358-360.
15. **Davydov Yu. M., In. M. Davydova, Egorov M. Yu. and others.** Numerical Research of Urgent Problems of Mechanical Engineering Both Mechanics of Continuous and Loose Environments by a Method of Large Particles. Vol.1 – Vol.5 / Editor by Yu. M. Davydov. – M.: NAAS, 1995. – 1658 p. (Russian).
16. **Nigmatulin R. I.** Bases of the Mechanics of Heterogeneous Environments. – M.: Nauka, 1978. – 336 p. (Russian).
17. **Davydov Yu. M.** Account of a Flow of Bodies of the Any Form by a Method of Large Particles. – Magazine of Calculus Mathematics and Mathematical Physics, 1971, vol.11, numbe 4, p.1056-1063. (Russian).